Plant Molecular Biology Reporter (2020) 38:538–553
https://doi.org/10.1007/s11105-020-01219-w

ORIGINAL PAPER

Transient Sub-cellular Localization and In Vivo Protein-Protein Interaction Study of Multiple Abiotic Stress-Responsive AteIF4A-III and AtALY4 Proteins in *Arabidopsis thaliana*

Indrani Baruah[1,2] · Geetanjali Baruah[3] · Jagajjit Sahu[4] · Dhanawantari L. Singha[1] · Hariprasanna Dekaboruah[1,2] · Natarajan Velmurugan[2,5] · Channakeshavaiah Chikkaputtaiah[1,2]

Published online: 11 May 2020

Abstract

Major abiotic stress factors such as drought, salinity, hypoxia, and extreme temperatures along with rapid global climate change have had a huge negative impact on agricultural productivity. Understanding the abiotic stress-responsive molecular mechanisms and its associated proteins is extremely important to advance our knowledge towards developing multiple abiotic stress tolerance in plants. Firstly, basic understanding at transient level would be a vital foundation to accomplish this goal. Therefore, our present study aimed at understanding the sub-cellular localization of Eukaryotic Initiation Factor 4A-III (AteIF4A-III), a key DEAD-box RNA helicase, and Always Early 4 (AtALY4), an mRNA export factor, and their in vivo protein-protein interaction with major abiotic stress–associated proteins under control and multiple abiotic stress conditions. AteIF4A-III and AtALY4 were localized to the nucleus as evident by transient protoplast assay. AteIF4A-III has shown strong interaction with a negative regulator of multiple abiotic stresses, Stress Response Suppressor 1 (AtSTRS1) in Bi-FC assay. Further, the flow cytometry analysis has shown the strong interaction between them. Interestingly, under multiple abiotic stress treatment, the interacting partners were rapidly re-localized from nucleus to cytoplasm and cytoplasmic space. Similar results were observed when N- and C-terminal fusions of AteIF4A-III and AtALY4 treated under multiple abiotic stresses. Our study reveals that AteIF4A-III, AtALY4, and abiotic stress–associated protein AtSTRS1 are among the key proteins associated with multiple abiotic stress responses in plants.

Keywords DEAD-box RNA helicases · Multiple abiotic stresses · Protein-protein interaction · Re-localization · AteIF4A-III · AtALY4

Key Message AteIF4A-III, a key plant DEAD-box RNA helicase; STRS1, an abiotic stress negative regulator; and AtALY4, an mRNA export factor are the key proteins associated with multiple abiotic stress responses in plants. The study signifies its implication in understanding tolerance to multiple abiotic stresses in plants.

Electronic supplementary material The online version of this article (https://doi.org/10.1007/s11105-020-01219-w) contains supplementary material, which is available to authorized users.

✉ Channakeshavaiah Chikkaputtaiah
channakeshav@neist.res.in

[1] Biotechnology Group, Biological Sciences and Technology Division, CSIR-NEIST, Jorhat, Assam 785006, India

[2] Academy of Scientific and Innovative Research (AcSIR), CSIR-NEIST Campus, Jorhat, Assam 785006, India

[3] Environment Division, Assam Science Technology and Environment Council (ASTEC), Bigyan Bhawan, Guwahati, Assam 781005, India

[4] DBT-North East Centre for Agricultural Biotechnology (DBT-NECAB), Assam Agriculture University, Jorhat, Assam 785013, India

[5] Biological Sciences Division, CSIR-NEIST Branch Laboratory-Itanagar, Naharlagun, Arunachal Pradesh 791110, India

Introduction

Plants are sessile organisms which endure numerous environmental adversities throughout its life span. Food security for the growing world population still remains a major problem, since conflict and climate-related shocks are associated with food crisis (Food and Agricultural organization, FAO 2017). Generally in plants, a large number of genes get activated as a response mechanism to abiotic stresses at transcriptional level, and the corresponding products are anticipated in activation of complex stress tolerance mechanisms (Barak and Farrant 2016; Han et al. 2019). In the current scenario, molecular breeding and biotechnology have emerged as powerful tools to identify abiotic stress-responsive genes and their molecular interconnections (Donoghue et al. 2011; Wang et al. 2018; Yadav and Tuteja 2019). Several novel genomic approaches like CRISPR/Cas9, CRISPR/Cpf1, TALEN, QTLs, ZFN, TILLING, microarray, ESTs, and SNPs certainly help in deciphering the cellular and molecular mechanism involved in multiple abiotic stress responses (Baruah et al. 2017; Chikkaputtaiah et al. 2017; Debbarma et al. 2019; Marwein et al. 2019). DEAD-box RNA helicases are the members of a large protein family called DEAD-box family proteins. Such helicases are found in most of the prokaryotic as well in eukaryotic organisms (Slaine et al. 2017; Tao et al. 2018; Ghosh 2019). DEAD-box proteins have gained importance recently for their multiple abiotic stress responses (Zhu et al. 2015; Liu et al. 2016; Baruah et al. 2017; Shivakumara et al. 2017; Nawaz et al. 2018a, b; Nguyen et al. 2018; Nawaz and Kang 2019). Recent studies have shown that overexpression of eIF4A under stress-inducible *Arabidopsis rd29A* promoter in groundnut showed improved tolerance against salinity, oxidative, and drought stress conditions (Rao et al. 2017). Exon junction complex (EJC) involved in post-transcriptional regulation including cytoplasmic localization, nonsense-mediated mRNA decay (NMD), and mRNA intracellular export in association with MAGO NASHI (MAGOH) and Y14 proteins (Yang et al. 2016). AteIF44AIII has been reported to be co-localized with MAGOH-Y14 in the nuclear region by interacting with an ortholog of the core EJC component, Always early RNA export factor (ALY/Ref) (Koroleva et al. 2009a, b). Localization shift has been observed to nucleolus and splicing speckles under hypoxia stress condition which suggests stress responsiveness of AteIF4A-III (Koroleva et al. 2009a, b) and its interaction with another EJC core component (AtALY4). AtALY4 or disco-interacting protein 2 (DIP2) is a sub-type of ALY-like DEAD-box RNA helicase which acts as an mRNA export factor from nucleus and protein remodeler (Pfaff et al. 2018). There are four ALY1 to ALY4 proteins commonly found in root and leaf cells of *Arabidopsis thaliana*. Research findings have revealed that AtALY4 ortholog of NbALY916 participates in multiple Nep1Mo (a Nep1-like protein from *Magnaporthe oryzae*)-triggered responses like stomatal closure, hypersensitivity cell death, and defense-related gene expression (Teng et al. 2014). Re-localization of nuclear ALY protein has been triggered by Tomato Bushy Stunt Virus P19 Pathogenicity Protein which shows biotic stress responsiveness of ALY proteins (Uhrig et al. 2004). Similarly, Stress Response Suppressor 1 (STRS1) has been reported as a negative regulator of abiotic stress response in plants and its sub-cellular localization in the nucleus through transient protoplast assay (Khan et al. 2014). The mutation of STRS1 enhanced the expression of the gene encoded for transcriptional activators DREB1A/CBF3 and DREB2A under salt, osmotic, and heat stress condition (Kant et al. 2007). Therefore, these scientific efforts suggest that there could be a regulatory network connecting AteIF4A-III, a DEAD-box gene, AtALY4, an mRNA export factor, and major stress-associated proteins intervening a key role in multiple abiotic stress responses. There have been many on-going works targeted to overcome single or dual stresses, but what plants experience in nature is the cumulative effect of the multiple abiotic stresses. Therefore, the need of the current agricultural scenario is to formulate research strategies to understand basic multiple abiotic stress responses in model plant system through cell biological and genetic approaches. Translation and adaptation of these strategies would help to develop crops which are multiple stress–tolerant to sustain the yield under adverse climatic change. Based on the recent findings of different DEAD-box proteins and known stress-associated proteins in abiotic stress response, we performed a systematic sub-cellular localization of AteIF4A-III and AtALY4, and their in vivo protein-protein interaction with abiotic stress–associated proteins such as AtSTRS1, Argonaute RISC component 4 (AtAGO4), Stress Response Suppressor 2 (AtSTRS2), and Chromatin Binding Factor (AtCBF5). The in vivo transient assays were performed in the *A. thaliana* protoplasts under normal and multiple abiotic stress conditions. The localization and interaction of these proteins were taking place at the nucleus, while we observed a rapid re-localization of these proteins from nucleus to cytoplasm and cytoplasmic space under multiple abiotic stress treatments. Flow cytometry analysis revealed the strong interaction of AteIF4A-III and AtSTRS1 proteins. Taken together, our study reveals that AteIF4A-III, AtALY4, and abiotic stress–associated protein AtSTRS1 are the key proteins associated with multiple abiotic stress responses in plants. Our findings in the model plant are highly significant in genetic improvement of crops to develop multi-stress tolerance by targeting these multi-stress-responsive genes.

Materials and Methods

Designing Gateway Cloning Constructs for Sub-cellular Localization and Split-YFP Protein-Protein Interactions

For sub-cellular localization of AteIF4A-III and AtALY4 proteins, N-terminal and C-terminal constructs were generated through Gateway cloning approach (Fig. S1a and c) as per manufacturer's instructions (Invitrogen). The positive entry clones were screened through colony PCR using kanamycin-specific primers. For the localization study, the entry clones of AteIF4A-III and AtALY4 were cloned into binary expression vectors, pENSG-YFP-P35S and pEXSG-YFP-P35S, to create N-terminal and C-terminal constructs through LR Clonase reaction. Whereas, for the interaction study, entry clones of AteIF4A-III, AtALY4, AtSTRS1, AtSTRS2, AtCBF5, and AtAGO4 were cloned into split-YFP vectors, pE-SPYNE and pE-SPYCE, with 35S promoter (Fig. S1b and d). The expression clones were selected by screening through amplification of the colonies with ampicillin-specific primers as well as restriction analysis. The N- and C- terminal constructs of AteIF4A-III and AtALY4 were used for sub-cellular localization study, and the spilt-YFP constructs were used for protein-protein interaction study. List of primers used in this study are given in Table S1.

Protoplast Isolation and Transient Abiotic Stress Assays in *Arabidopsis thaliana*

WT (Col-0) seeds of *Arabidopsis thaliana* was surface sterilized and inoculated on ½ MS medium by following the protocol of Rivero et al. (2014). These plates were kept in dark at 4 °C for 2 days as stratification period to break dormancy of the seeds. Then, these plates were kept in the tissue culture chamber at 23 °C temperature, 70% humidity, and 16 h light/8 h dark photoperiod. After 1 week, the germinated 4-leaf stage seedlings were transferred into the germination soil with cocopeat:vermiculite:perlite in 4:1:1 ratio. The soil-transferred *Arabidopsis* seedlings were shifted to plant growth chamber at 23 °C temperature, 70% humidity, and 16 h light/8 h dark photoperiod optimal growth conditions. The 3–4 weeks old seedlings were chosen for isolation of protoplasts. The protoplast isolation and PEG-mediated transfection was carried out as per protocol of Yoo et al. (2007). Young leaves were cut with sterile scalpel into 0.5–1-mm leaf strips and digested in enzyme solution of 1.5% (wt./vol) cellulase and 0.4% (wt./vol) macerozyme R10 for 4 h on a shaker at 40 rpm. After digestion, the protoplasts were purified by washing with W5 solution and passing through 70 μm nylon mesh. The isolated protoplasts were finally resuspended into MMG solution. For transformation of protoplasts, 100 μl of purified protoplasts were taken in each tube for each construct. To each tube, 10 μl of localization constructs of eIF4A-III and ALY4 were added individually. For split-YFP assay, 10 μl of the split-YFP constructs were added pairwise in separate tubes containing 100 μl of protoplasts. To this mixture, 110 μl of PEG solution was added and mixed gently. The tubes were incubated at room temperature for 15 min. A total of 400 μl of W5 solution was added and inverted few times to stop the PEG transfection process. The tubes were then centrifuged at 100 g for 2 min at room temperature. Supernatant was discarded, and the pellet was dissolved in 1 ml of W1 solution. All the transformed protoplasts were incubated at 25 °C in the dark for 16 h. Several literatures have shown that the plant protoplasts were found to be viable after exposing to salt, drought, and oxidative stress conditions (Keunen et al. 2011; Kiełkowska et al. 2019; Kollárová et al. 2019). For our transient multiple abiotic stress assays, salt, drought and hypoxia stress conditions were imposed by treating the transformed protoplast cells with 200 mM NaCl, 20% PEG-6000, and 100 mM sodium azide, respectively for 120 min (Zhu et al. 2015; Hasanuzzaman et al. 2016; Koroleva et al. 2009b). The treated protoplasts were observed under confocal microscopy after 120 min. The protoplasts with localization and split-YFP constructs were stained with DAPI and observed under × 63 oil emersion using a Leica TCS SP8 inverted confocal microscope. The image acquisition was done through Leica LAS-X software and ImageJ software. FITC, EYFP PMT, and DAPI detectors were used for imaging. YFP fluorescence was detected with 488 nm and 514 nm excitation; emission wavelengths range 505–530 nm; DAPI fluorescence was detected with 405 excitations and 507–530 nm. The chlorophyll auto-fluorescence was analyzed with 555 nm excitation and > 650 nm emission. In the split-YFP interaction assays, the target proteins with pE-SPYNE and pE-SPYCE were fused with two non-fluorescent YFP protein halves (ESM.1). When the two target proteins interact, the YFP protein halves also come into proximity and emit yellow fluorescence (Ohad et al. 2007). Therefore, in our study, the positive split-YFP interactions are expected to show yellow fluorescent signals under confocal microscopy. This experiment of localization and split-YFP assay was performed three times independently.

Quantification of Split-YFP In Vivo Protein-Protein Interaction through Flow Cytometry

Protein-protein interaction was observed by performing Bi-FC assay with the split-YFP constructs generated through Gateway cloning approach. The split-YFP constructs were transformed into fresh mesophyll protoplast and incubated for 16 h at 25 °C. The protein-protein interaction was quantified with the help of flow cytometry analysis approach using CytoFLEX-S flow cytometer (Beckman Coulter, USA). YFP signal in the protoplast samples were detected by using FITC-YFP florescence detector with 488 nm excitation and 507–

530 nm emission range. Protoplasts transformed with pE-SPYE × pE-SPYCE without any fused proteins (empty vector) were taken as negative control. In flow cytometry, cytometric characteristics of the cells or particles can be measured through light scattered and emitted by the cells or particles (Herzenberg et al. 2006). There are two major light scattering processes to measure signal scattered by cells which are forward scatter (FSC) and side scatter (SSC). The FSC is known to provide information on cell or particle sizes, whereas the side SSC provides information on internal components of the cell or particle (da-Silva et al. 2012). Dot plot with FSC vs SSC shows the total cell events. Each spot in the dot plot represents a cell. To avoid cell debris, media contamination, or cell doublets, the single cells can be gated from the FSC vs SSC dot plot. The gated region of this dot plot is considered as 100% viable cell population. This gated region can be analyzed on a different dot plot having FITC-YFP fluorescence intensity vs SSC to get information of the fluorescence intensity of the internal component of the cells. For normalization, the fluorescent population will deviate and form a separate cluster from the non-fluorescent negative control cluster (Herzenberg et al. 2006). In the FITC-YFP fluorescence intensity vs SSC dot plot, the cells showing YFP fluorescence will shift towards the right side of the plot, and the percentage of event the fluorescent population will be counted automatically by flow cytometry. Similarly, the fluorescent and non-fluorescent cell clusters can be observed in peak form in the histogram plot. Percent (%) represents how many protoplast cells have shown YFP positive signal out of the total number of cells tested in flow cytometry. We used protoplasts transformed with empty split-YFP vector combination (pE-SPYCE X pE-SPYNE) and empty expression vector (pENSG-YFP) as negative controls for quantification of Bi-FC analysis and sub-cellular localization analysis through flow cytometry, respectively.

Phylogenetic Analysis and Protein-Protein Interaction Network

Phylogenetic analysis identifies the closeness between sequences and is an indicative of the functional relationship among them. Molecular Evolutionary Genetics Analysis (MEGA 7.0.14) software was used to perform the phylogenetic analysis by taking the protein sequences of AteIF4A-III DEAD-box RNA helicase and related stress-associated proteins such as AtALY4, AtAGO4, AtSTRS1, AtSTRS2, and AtCBF5 as input. At first, the protein-protein interaction information was extracted by AraNet V2 which provides a base to predict probabilistic functional network for *A. thaliana*. The selected DEAD-box proteins were searched for the corresponding locus identifiers, and these IDs were fed into AraNet to build an interaction network. The interaction data obtained from the flow cytometry were customized in an input file format for Cytoscape tool. Both information from AraNet and flow cytometry were then merged using "merge" function in R. This was used as the final input in the Cytoscape V 3.5.1 to construct a network representing interactions between the selected proteins.

Results

Sub-cellular Localization of AteIF4A-III and AtALY4 Under Normal and Multiple Abiotic Stress Conditions

Gateway constructs were designed by Advanced Gateway cloning method (Fig. S1a and c). Under normal (unstressed) condition, AteIF4A-III was found to be localized in the nucleus in both N-terminal and C-terminal fusion constructs (Fig. 1a and Fig. S2a). The merged image showed co-localization of DAPI and YFP signals confirming the nuclear localization of AteIF4A-III (Fig. 1c and Fig. S2c). Hypoxia stress condition lead to re-localization of YFP-AteIF4A-III and AteIF4A-III-YFP from nucleus to cytoplasmic space (Fig. 1f and Fig. S2f). Under drought condition, rapid re-localization of YFP-AteIF4A-III and AteIF4A-III-YFP to all over the cytoplasm and cytoplasmic peripheral region was observed (Fig. 1k and Fig. S2k). Under salinity condition, YFP-AteIF4A-III re-localized to cytoplasmic peripheral region (Fig. 1p), and in case of AteIF4A-III-YFP, the YFP signals were evenly distributed in the cytoplasm (Fig. S2p). Similarly, under unstressed condition, sub-cellular localization of YFP-AtALY4 and AtALY4-YFP were observed in the nuclear region as DAPI stained cells co-localized with the YFP signal expressing in the nucleus (Fig. 2a–c and Fig. S3a-c). Under hypoxia stress condition, re-localization of YFP-AtALY4 and AtALY4-YFP were observed from the nucleus to cytoplasm and cytoplasmic space (Fig. 2f–j and Fig. S3f-j). However, clear localization shift of YFP-AtALY4 and AtALY4-YFP towards the cytoplasmic periphery was observed under drought stress condition (Fig. 2k and Fig. S3k). Under salinity condition, YFP-AtALY4 signal was evenly distributed in the cytoplasm (Fig. 2p–t). On the other hand, AtALY4-YFP was observed in the cytoplasm and also in the nucleus with a poor YFP signal (Fig. S3p-t). In order to exclude the false signal, empty vectors, pENSG-YFP and pEXSG-YFP, transformed into protoplasts were used as negative controls for N- and C-terminal constructs of AteIF4A-III and AtALY4. Both the negative controls did not show any YFP signals (Figs. 1u, 2u, Fig. S2u, and Fig. S3u). The in vivo sub-cellular localization experiment was conducted thrice, and the results were found to be consistent.

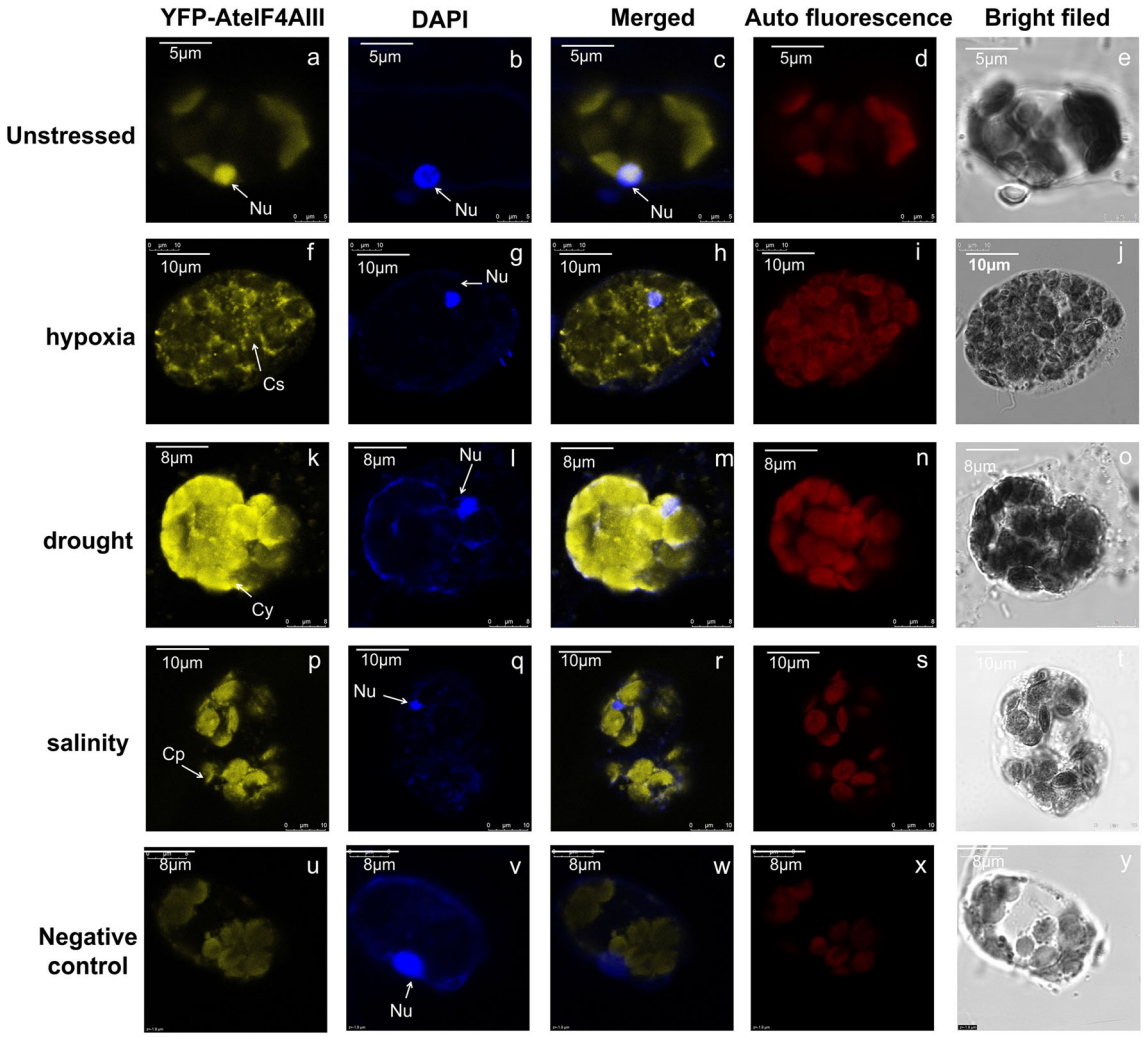

Fig. 1 Sub-cellular localization of YFP-AteIF4AIII under normal (unstressed) and multiple abiotic stress conditions. YFP-AteIF4AIII localized in the nucleus with strong YFP signal under normal condition (a–e). Under hypoxia stress (100 mM Sodium Azide) for 120 min, YFP-AteIF4AIII re-localizes from nucleus to cytoplasmic space (f–j). Under drought stress (20% PEG) for 120 min, YFP-AteIF4AIII re-localizes to cytoplasm (k–o). Under salinity stress (200 mM NaCl) for 120 min, YFP-AteIF4AIII re-localizes to cytoplasmic periphery (p–t). pENSG-YFP empty vector as negative control (u–y). Nu, nucleus; Cy, cytoplasm; Cp, cytoplasmic periphery. Scale bars, a–e = 5 µm; k–o and u–y = 8 µm; f–j and p–t = 10 µm. About fifty cells were observed under confocal microscopy from which thirty cells have shown the effects. The experiment was repeated thrice, and the results were consistent

In Silico Analysis of Protein Partners of DEAD-Box RNA Helicases and Stress-Associated Proteins

The phylogenetic tree revealed that AteIF4A-III, AtALY4, AtSTRS1, and AtSTRS2 are falling in one cluster, whereas AtCBF5 and AtAGO4 were forming a different cluster (Fig. S4). This indicates that AteIF4A-III, AtALY4, AtSTRS1, and AtSTRS2 might be functionally related to each other. However, AtCBF5 and AtAGO4 are functionally distant from the first cluster. The bootstrap value for the node between AteIF4A-III and AtSTRS2 is 99, for the node sharing AteIF4A-III, AtSTRS1, and AtSTRS2 is 100, and for the node sharing AteIF4A-III, AtSTRS1, AtSTRS2, and AtALY4 is 83 (Fig. S4). The bootstrap value of 100% for the node sharing by AteIF4A-III, AtSTRS2, and AtSTRS1 supports the significance of the phylogenetic data and suggests a strong accuracy of the functional association prediction. We performed in silico predictions of protein interactors using stringsdb and AraNet V2 bioinformatics resources. However, the AraNet V2 was identified as the best as it provides a probabilistic functional gene network for *Arabidopsis thaliana* incorporated with large-scale experimental data and improved data analysis algorithms. The AraNet V2 database is more specific to *Arabidopsis thaliana*. Most of the protein-protein interaction databases provides gene-gene co-expression information as it establishes the prediction of interaction strongly. So, the in silico protein interactions in this study are from the well-established database AraNet V2. Protein-protein interactions among AteIF4A-III,

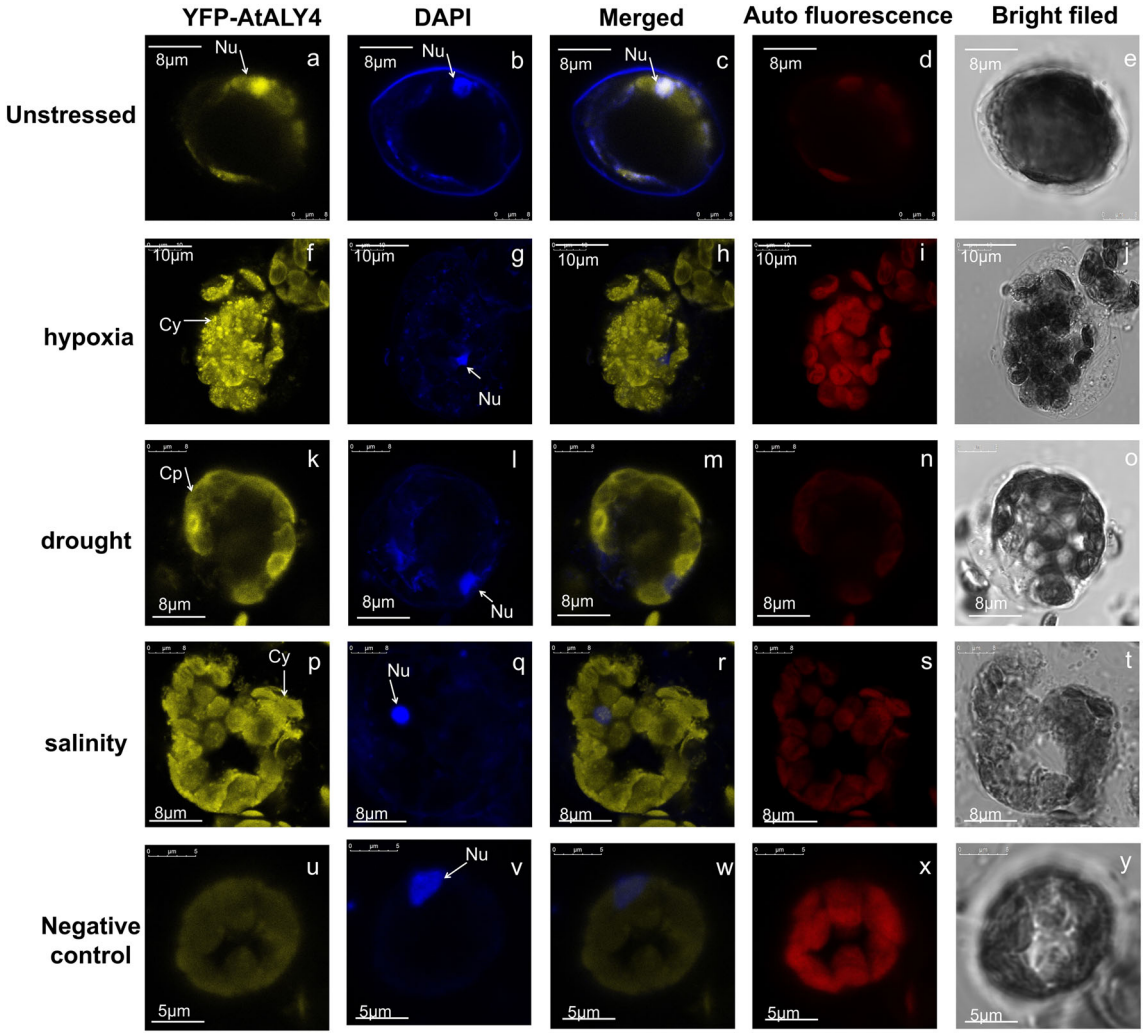

Fig. 2 Sub-cellular localization of YFP-AtALY4 under normal (unstressed) and multiple abiotic stress conditions. YFP-AtALY4 localized in the nucleus with strong YFP signal under normal condition (a–e). Under hypoxia stress (100 mM Sodium Azide) for 120 min, YFP-AtALY4 re-localizes from nucleus to cytoplasm (f–j). Under drought stress (20% PEG) for 120 min, YFP-AtALY4 re-localizes to cytoplasmic periphery (k–o). Under salinity stress (200 mM NaCl) for 120 min, YFP-AtALY4 re-localizes to cytoplasm (p–t). pENSG-YFP empty vector as negative control (u–y). Nu, nucleus; Cy, cytoplasm; Cp, cytoplasmic periphery. Scale bars, a–e and k–t = 8 μm; f–j = 10 μm; u–y = 5 μm. About fifty cells were observed under confocal microscopy from which twenty five cells have shown the effects. The experiment was repeated thrice, and the results were consistent

AtALY4 (DIP2), AtCBF5 or Nucleolar Protein (NAP57), AtSTRS1, AtAGO4, and AtSTRS2 were identified using the AraNet V2 software in the form of a network (Fig. S5). There are interactions among AteIF4A-III, AtSTRS1, and AtCBF5 (NAP57). AtSTRS1 also interacts with AteIF4A-III, AtCBF5, and AtSTRS2; AtSTRS2 interacts with AtSTRS1 and AtCBF5; AtALY4 (DIP2) interacts with AtCBF5. To compare and get more insight into the in silico and in vivo protein-protein interactions, the merged (both results from AraNet and flow cytometry) network was analyzed using Cytoscape (Fig. 6). The network is of 6 nodes and 10 edges which represents the 6 proteins and 12 interactions (merged into 10 edges) among them. For the in silico network, the search was restricted to only the 6 selected proteins based on the experimental data. The network inferred that the interaction between AteIF4A-III and AtSTRS1; AtSTRS2 and AtSTRS1 were supported by both computer-aided as well as in vivo experiments. Consistent with our in vivo results, the in silico analysis also have shown direct interaction of AteIF4A-III with AtSTRS1 (Fig. 6). AteIF4A-III also showed a strong interaction with AtALY4 in our in vivo study which is in accordance with Koroleva et al. (2009b). Surprisingly however, in silico analysis did not show a direct interaction of AteIF4A-III with AtALY4 or AtAGO4 with AteIF4A-III, and AtSTRS1 or AtALY4 with AtSTRS1. On the other hand, proteins such as these were connected by edges based on in vivo findings. The AtCBF5 was connected to

AteIF4A-III, AtSTRS2, AtALY4, and AtSTRS1 directly with edges predicted only using in silico method. The network from the AraNet shows the probability of interaction of AteIF4A-III DEAD-box RNA helicase with AtCBF5 and AtSTRS1 stress-associated proteins (Fig. S5). Similarly, it shows interaction prediction of AtALY4 with AtCBF5 stress-associated proteins. Comparison of in silico and in vivo protein-protein interactions of AteIF4A-III, AtALY4, and stress-associated proteins is given in Table 2.

In Vivo Protein-Protein Interaction of DEAD-Box RNA Helicases with Other Stress-Associated Proteins through Split-YFP Assay Under Normal and Multiple Abiotic Stress Conditions

For transient protein-protein interaction study, target proteins were fused with two non-fluorescent protein halves of YFP (Fig. S1b). Earlier studies have shown that AteIF4A-III and AtSTRS1 individually play a very important role in abiotic stress response (Kant et al. 2007; Koroleva et al. 2009b; Pascuan et al. 2016). Therefore, we hypothesized that the protein-protein interaction between AteIF4A-III and AtSTRS1 might reveal their functional interconnection under multiple abiotic stress conditions. In order to analyze their interaction pattern, in vivo split-YFP constructs of AteIF4A-III and AtSTRS1 were generated and visualized in both the directions, i.e., AteIF4A-III$^{pE\text{-}SPYCE}$ × AtSTRS-1$^{pE\text{-}SPYNE}$ and AteIF4A-III$^{pE\text{-}SPYNE}$ × AtSTRS-1$^{pE\text{-}SPYCE}$. The strong protein-protein interaction between AteIF4A-III and AtSTRS1 were observed in both the directions, and the interaction was localized in the nucleus under normal conditions (Figs. 3a and 4a). DAPI signal co-localized with the YFP signal in both the directions confirmed the strong nuclear localization of the positive interactors (Figs. 3b and 4b). Under hypoxia stress condition, the AteIF4A-III and AtSTRS1 positive interactors were re-localized from the nucleus to cytoplasmic space in both the directions (Figs. 3f and 4f). Under drought stress condition, the AteIF4A-III and AtSTRS1 positive interactors were rapidly re-localized from the nucleus to cytoplasmic space and cytoplasmic periphery in both the directions (Figs. 3k and 4k). Similarly, under salinity condition, the AteIF4A-III and AtSTRS1 positive interactors were re-localized to the entire cytoplasm in both the directions (Figs. 3p and 4p). In order to exclude the possibility of artifacts or false positives, different sets of negative controls were used. The combination of empty split-YFP vectors, pE-SPYNE and pE-SPYCE, transformed into protoplasts was used as standard negative controls for testing all the interaction patterns (Figs. 3u–y and 4u–y). For first combination of AteIF4A-III and AtSTRS1 binding partners (AteIF4A-III$^{pE\text{-}SPYCE}$ X AtSTRS1$^{pE\text{-}SPYNE}$), AteIF4A-III$^{pE\text{-}SPYCE}$ × SlXSP10$^{pE\text{-}SPYNE}$ was used as first set of negative control (Fig. 3a1–e1), while AtSTRS1$^{pE\text{-}SPYNE}$ × SlXSP10$^{pE\text{-}SPYCE}$ was used as second set of negative control (Fig. 3f1–j1). For second combination of AteIF4A-III and AtSTRS1 binding partners (AteIF4A-III$^{pE\text{-}SPYNE}$ × AtSTRS1$^{pE\text{-}SPYCE}$), AteIF4A-III$^{pE\text{-}SPYNE}$ × SlXSP10$^{pE\text{-}SPYCE}$ was used as first set of negative control (Fig. 4a1–e1), while AtSTRS1$^{pE\text{-}SPYCE}$ × SlXSP10$^{pE\text{-}SPYNE}$ was used as second set of negative control (Fig. 4f1–4j1). SlXSP10 is a xylem sap protein of tomato (*Solanum lycopersicum*) known to be involved in Fusarium wilt disease responses (Krasikov et al. 2011). In all the negative controls tested, no YFP signal was observed. The results indicate that AteIF4A-III and AtSTRS1 are the positive binding partners in vivo. The in vivo split-YFP interaction experiments under normal and multiple abiotic stress conditions were repeated thrice, and the results were found to be consistent.

Quantification of Sub-cellular Localization and Protein-Protein Interaction of In Vivo Positive Interacting Proteins

The sub-cellular localization of eIF4A-III and ALY4 were quantified by flow cytometry. eIF4A-III-YFP showed 37.16% YFP fluorescence (Fig. 5a, b), and YFP-eIF4A-III showed 23.42% YFP fluorescence (Fig. 5c, d). Similarly, ALY4-YFP showed 32.29% YFP fluorescence (Fig. 5e, f), and YFP-ALY4 showed 38.06% YFP fluorescence (Fig. 5g, h). The empty expression vector pENSG-YFP transformed into *Arabidopsis* protoplasts used as negative controls showed only 0.08% of YFP fluorescence (Fig. 5m, n). The in vivo positive protein-protein interactions were quantified using flow cytometric analysis. The strong protein partner AteIF4A-III$^{pE\text{-}SPYNE}$ × AtSTRS-1$^{pE\text{-}SPYCE}$ showed 85.39% YFP fluorescence (Fig. 5i, j). The other interacting partner, AtSTRS-1$^{pE\text{-}SPYNE}$ × AteIF4A-III$^{pE\text{-}SPYCE}$, showed 84.90% YFP signal (Fig. 5k, l). A combination of empty split-YFP vectors, pE-SPYNE × pE-SPYCE, transformed into protoplasts that were used as a negative control did not show any YFP signal (Fig. 5o, p). The flow cytometry quantification results in comparison with negative controls indicate that the YFP signals observed in sub-cellular localization and in vivo protein-protein interactions were highly significant. Each quantification experiment of sub-cellular localization and in vivo protein-protein interaction was repeated thrice, and the results were found to be consistent.

Discussion

AteIF4A-III and AtALY4 Are Nuclear-Localized and Stress-Responsive Re-Localized to Cytoplasm

Sub-cellular localization of DEAD-box RNA helicase AtAteIF4A-III and putative mRNA export factor AtALY4

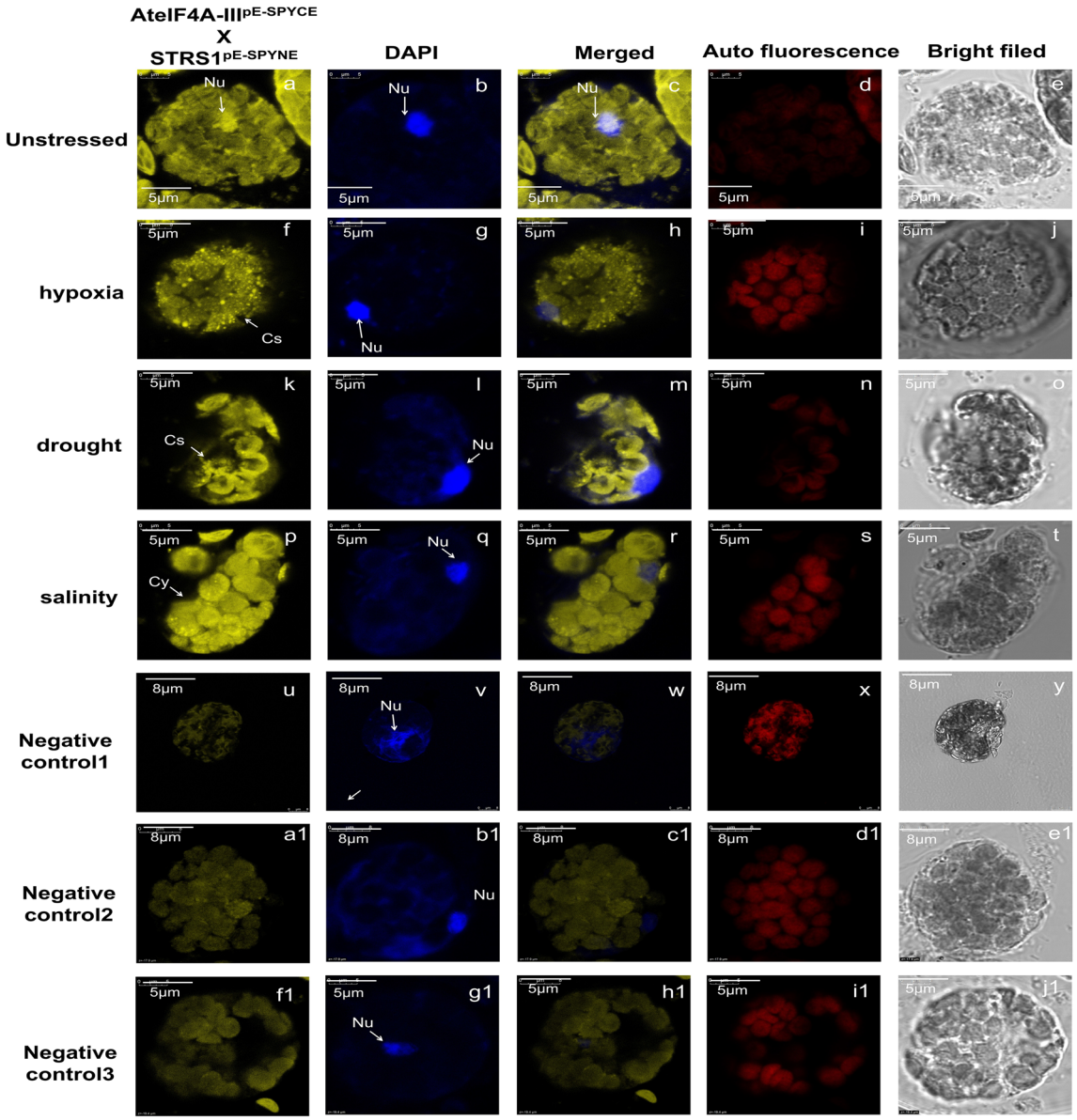

Fig. 3 In vivo protein-protein interaction of AteIF4A-III$^{pE\text{-}SPYCE}$ X AtSTRS1$^{PE\text{-}SPYNE}$ under normal (unstressed) and multiple abiotic stress conditions. AteIF4A-III$^{PE\text{-}SPYCE}$ X AtSTRS1$^{PE\text{-}SPYNE}$ interacting at nucleus under normal conditions (a–e), re-localized to cytoplasmic space under hypoxia stress (f–j), re-localized to cytoplasmic space under drought stress (k–o), re-localized to cytoplasm under salinity stress (p–t). pE-SPYCE X pE-SPYNE as standard negative control (u–y). AteIF4A-III$^{pE\text{-}SPYCE}$ X SlXSP10$^{pE\text{-}SPYNE}$ as first set of negative control (a1–e1). AtSTRS1$^{pE\text{-}SPYNE}$ X SlXSP10$^{pE\text{-}SPYCE}$ as second set of negative control (f1–j1). Nu, nucleus; Cs, cytoplasmic space; Cy, cytoplasm. Scale bars a–t = 5 µm; u–y and a1–e1 = 8 µm. About sixty cells were observed under confocal microscopy from which fifty cells have shown the effects. The experiment was repeated thrice, and the results were consistent

was performed to unveil their functional site under normal and multiple abiotic stress conditions. Sodium azide is an oxidative phosphorylation inhibitor which, by inhibiting mitochondrial respiration, causes depletion of intracellular ATP synthesis and creates hypoxia stress (Freye and Strobel 2018), whereas polyethylene glycol (PEG) has been considered as a drought stress inducer with no toxic effect (Hellal et al. 2017). Drought stress reduces the photosynthetic rate of plants by affecting photosynthetic pigments. Similarly, high concentration of NaCl creates salinity stress condition (Lycoskoufis et al. 2012). High concentrations of Na^+ and Cl^- ions disrupt K^+ and Ca^- nutrition and reduce plant growth with poor yield. Under normal condition, sub-cellular localization studies of YFP-AteIF4A-III and AteIF4A-III–YFP have revealed nuclear localization. Numerous cellular mechanisms are processed within the nucleus, which include cell cycle regulation, RNA processing, ribonucleotide proteins (RNP) biogenesis, telomerase activity, and stress-responsive signaling. The clear nuclear localization of AteIF4A-III suggests that the function of AteIF4A-III resides within the nucleus, and hence it is an

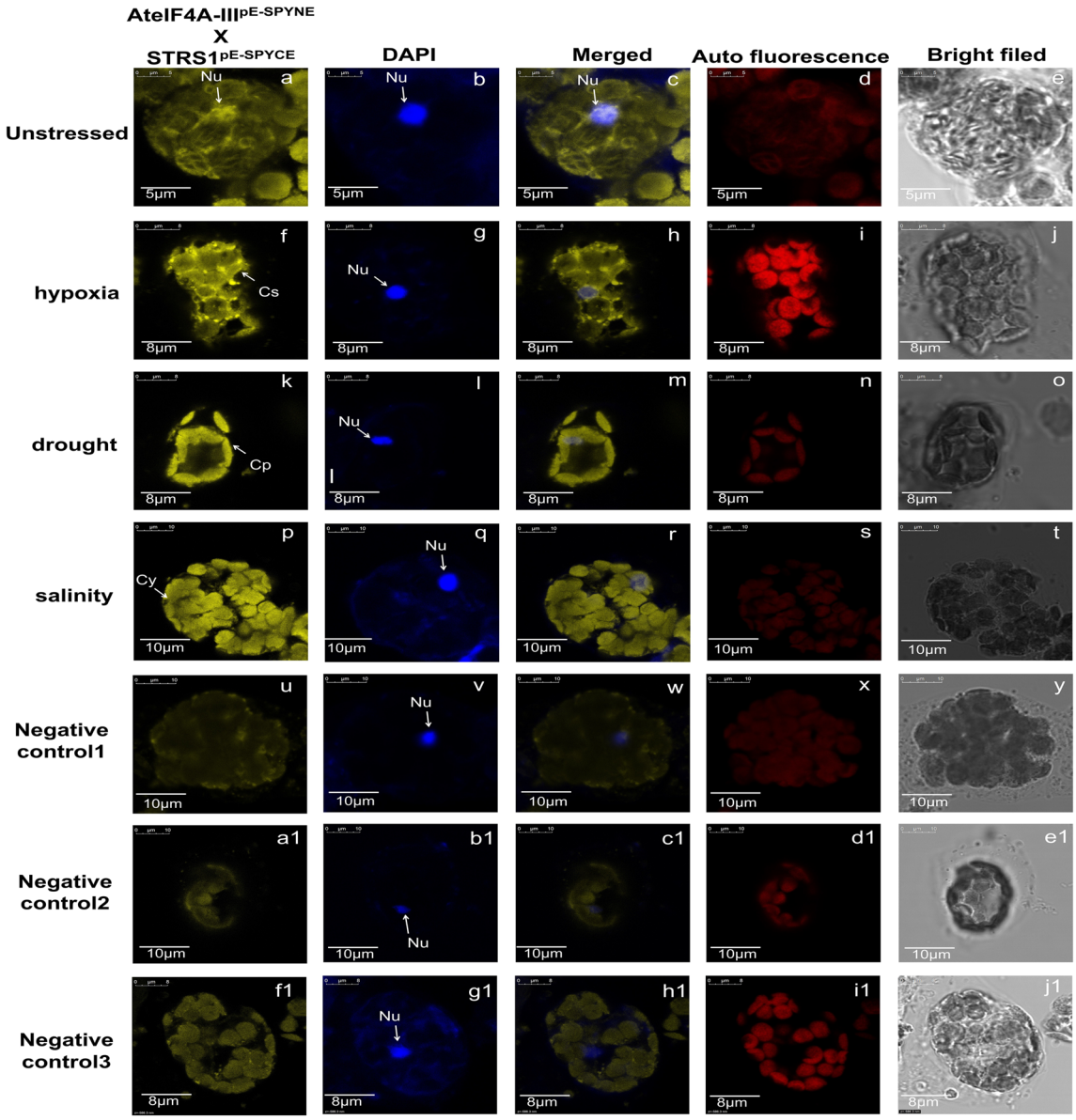

Fig. 4 In vivo protein-protein interaction of AteIF4A-III$^{PE\text{-}SPYNE}$ X AtSTRS1$^{PE\text{-}SPYCE}$ under normal (unstressed) and multiple abiotic stress conditions. AteIF4A-III$^{PE\text{-}SPYNE}$ X AtSTRS1$^{PE\text{-}SPYCE}$ interacting at nucleus under normal conditions (a–e), re-localized to cytoplasmic space under hypoxia stress (f–j), re-localized to cytoplasmic periphery under drought stress (k–o), re-localized to cytoplasm under salinity stress (p–t). pE-SPYCE X pE-SPYNE as standard negative control (u–y). AteIF4A-III$^{PE\text{-}SPYNE}$ X SlXSP10$^{PE\text{-}SPYCE}$ as first set of negative control (a1–e1), AtSTRS1$^{PE\text{-}SPYCE}$ X SlXSP10$^{PE\text{-}SPYNE}$ as second set of negative control (f1–j1). Nu, nucleus; Cp, cytoplasmic periphery; Cy, cytoplasm. Scale bar, a–e = 5 μm; f–o and f1–j1 = 8 μm; p–y and a1–e1 = 10 μm. About sixty cells were observed under confocal microscopy from which forty-five cells have shown the effects. The experiment was repeated thrice, and the results were consistent

active participant of several important cellular events. OsRH2 and OsRH34 are paralogous genes of AteIF4A-III found in rice which play an important role in growth and development by regulating plant height, pollen, and seed germination (Huang et al. 2016). These two genes are also found as a core component of the EJC complex just like AteIF4A-III which is a putative member of the EJC complex (Pierrat et al. 2017; Boisramé et al. 2019). Recent findings have also revealed the nuclear localization of AteIF4A-III and its importance in mRNA processing and pre-mRNA splicing (Koroleva et al. 2009a; Andreou and Klostermeier 2013). The import of "nuclear" proteins into the nucleus, especially TFs is a response to certain external stimuli (Vandromme et al. 1996). Lu et al. (2014) have shown that AteIF4A-III sub-cellular localization in tobacco and *A. thaliana* was centered in nucleoplasm, and there was a rapid localization shift of AteIF4A-III from the nucleoplasm to nucleolus and splicing speckles, under hypoxia and ethanol treatment. It shows that AteIF4A-III acts as stress response indicator under hypoxia condition, certain mRNA remains bound to AteIF4A-III and mRNA processing

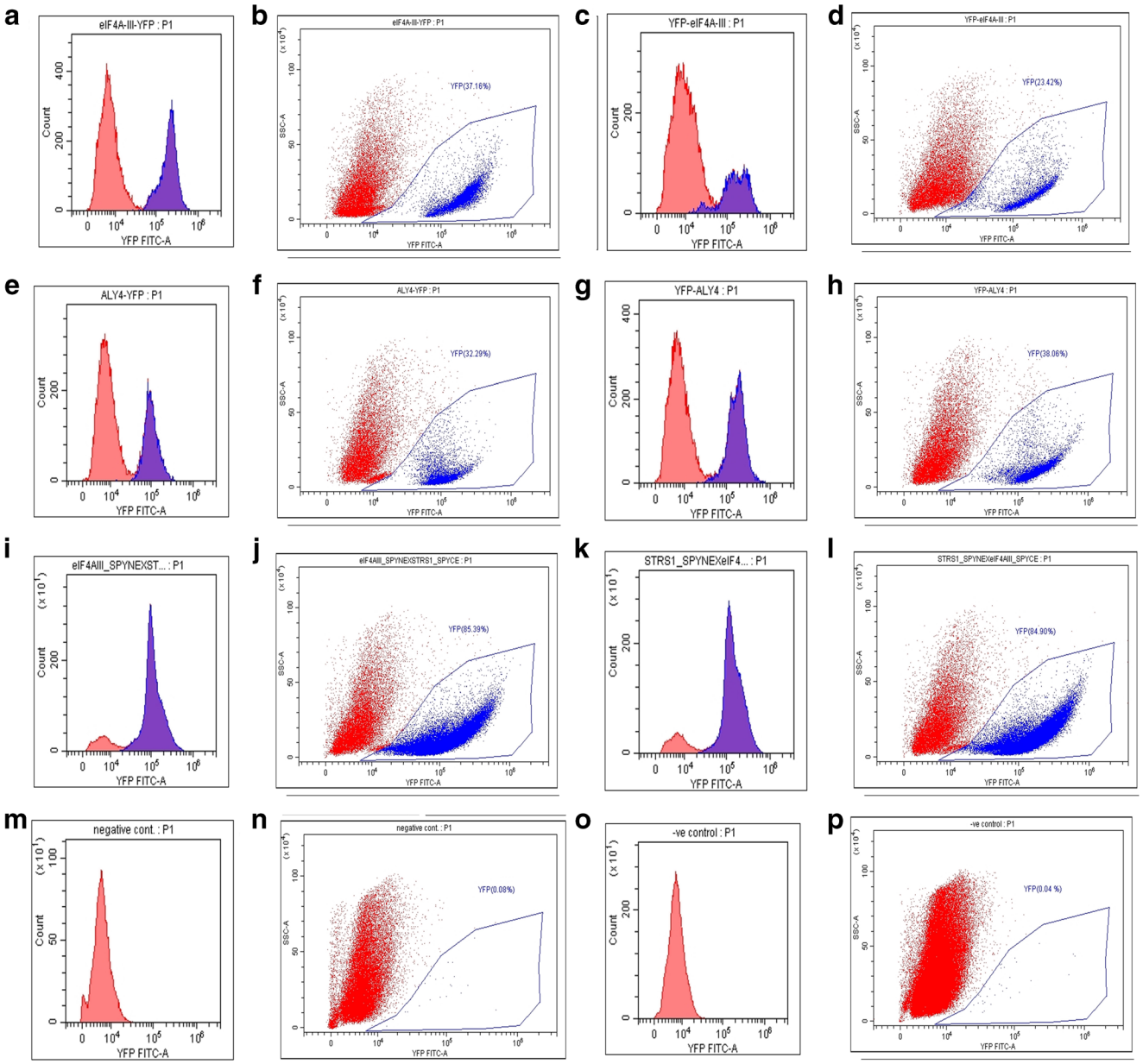

proteins. Thus, further translation process was suspended under a stressed condition. Depletion of intracellular ATP synthesis hampers the AteIF4A-III functions. In our study, important cellular biogenesis events were suppressed as AteIF4A-III shifted to the cytoplasmic space under hypoxia stress condition. Similarly, under drought stress condition, even distribution of AteIF4A-III was observed in the cytoplasm in this study. This localization shift suggests that under drought stress condition, AteIF4A-III might play some important role in regulation or activation of other stress-responsive proteins in the cytoplasm. Distribution of AteIF4A-III in cytoplasmic periphery and cytoplasm under salinity condition also indicates stress responsiveness of AteIF4A-III. From our results, it can be inferred that AteIF4A-III shifts its localization to cytoplasmic periphery and cytoplasm to lower the biogenesis events under different abiotic stress conditions. This might help the plant to survive under abiotic stresses with a minimal energy source. Transgenic groundnut with *eIF4A* gene from *Pennisetum glaucum* under rd29A stress-inducible promoter shows improved adaptation against salinity and drought stress conditions (Rao et al. 2017). In *A. thaliana*, four ALY protein orthologs ALY1, ALY2, ALY3, and ALY4 have shown differential sub-nuclear localization (Naturwissenschaften 2016). AtALY4 is known as a putative mRNA export factor which is involved in RNA processing and RNP biogenesis (Kammel et al. 2013; Teng et al. 2014; Boisramé et al. 2019). In our study, the sub-cellular localization result of AtALY4 under normal condition shows that the nucleus is the functional site of AtALY4 for its physiological function. In *Arabidopsis*, recent research work on AtALY4 revealed its functional

◀ **Fig. 5** Flow cytometry quantification of sub-cellular localizations and in vivo protein-protein interactions. **a** Histogram showing red colored peak as non-fluorescent and blue colored peak representing YFP fluorescent cells in eIF4A-III-YFP. **b** Dot plot showing eIF4A-IIII-YFP (blue color) shifting towards right side separating from non-fluorescent cell cluster (red color) with 37.16% YFP fluorescence. **c** Histogram showing red colored peak as non-fluorescent and blue colored peak representing YFP fluorescent cells in YFP-eIF4A-III. **d** Dot plot shows YFP- eIF4A-IIII (blue color) shifting towards right side separating from non-fluorescent cell cluster (red color) with 23.42% YFP fluorescence. **e** Histogram showing red colored peak as non-fluorescent and blue colored peak representing YFP fluorescent cells in ALY4-YFP. **f** Dot plot shows ALY4-YFP (blue color) shifting towards right side separating from non-fluorescent cell cluster (red color) with 32.29% YFP fluorescence. **g** Histogram showing red colored peak as non-fluorescent and blue colored peak representing YFP fluorescent cells in YFP-ALY4. **h** Dot plot shows YFP-ALY4 (blue color) shifting towards right side separating from non-fluorescent cell cluster (red color) with 38.06% YFP fluorescence. **i** Histogram showing red colored peak as non-fluorescent and blue colored peak representing YFP fluorescent cells in AteIF4A-III$^{PE\text{-}SPYNE}$ × AtSTRS1$^{PE\text{-}SPYCE}$ positive interactors. **j** Dot plot shows AteIF4A-III$^{PE\text{-}SPYNE}$ × AtSTRS1$^{PE\text{-}SPYCE}$ (blue color) shifting towards right side separating from non-fluorescent cell cluster (red color) with 85.39% YFP fluorescence. **k** Histogram showing red colored peak as non-fluorescent and blue colored peak representing YFP fluorescent cells in AtSTRS1$^{PE\text{-}SPYNE}$ × AteIF4A-III$^{PE\text{-}SPYCE}$ positive interactors. **l** Dot plot shows AtSTRS1$^{PE\text{-}SPYNE}$ × AteIF4A-III$^{PE\text{-}SPYCE}$ (blue color) shifting towards right side separating from non-fluorescent cell cluster (red color) with 84.90% YFP fluorescence. **m** Histogram showing only one red colored peak as non-fluorescent cells in pENSG-YFP empty vector transformed protoplasts as negative control for localization study. **n** Dot plot showing no shift of non-fluorescent cell cluster (red color) right side with 0.08% YFP fluorescence in negative control of localization. **o** Histogram showing only one red colored peak as non-fluorescent cells in pE-SPYNE × pE-SPYCE empty vector construct (negative control for split-YFP interaction study). **p** Dot plot shows no shift of non-fluorescent cell cluster (red color) right side with 0.04% YFP fluorescence in the negative control of split-YFP. Percent (%) represents how many protoplast cells have shown YFP positive signal out of the total number of cells tested in flow cytometry. Each experiment was conducted three times, and the results were found to be consistent

localization in the nucleus, and it has been found to be involved in nucleo-cytosolic mRNA transport, ovule, and flower development (Pfaff et al. 2018). Nucleo-cytoplasmic movement play an important regulatory barrier in gene expression of control points (Vandromme et al. 1996). Just like AteIF4A-III, exposure of different stress conditions also affects the normal localization of AtALY4. Under hypoxia condition, the shift from nucleus to cytoplasm and cytoplasmic space indicates the stress responsiveness of AtALY4. However, exposure to drought and saline condition shifts AtALY4 from the nucleus to cytoplasmic periphery and to cytoplasm with poor signal in nucleus. This localization shift suggests that AtALY4 is involved in the cellular machinery like RNA biogenesis through mRNA export in the nucleus. AtALY4 moves from the nucleus to the cytoplasmic periphery and to cytoplasm to slow down the biosynthesis processes to escape the stressed condition. Recent research reports showed that the localization shift from one to another cell organelle under abiotic stress conditions indicates their involvement in stress responses. Powers et al. (2019) found that auxin response factor (ARF) nucleo-cytoplasmic partitioning regulates auxin responsiveness that confers cellular competence for auxin signaling. VASCULAR PLANT ONE-ZINC FINGER 2 (VOZ 2) was found to be dispersed in the cytoplasm but re-localized to the nucleus as heat stress response and act as *DREB2A* transcriptional suppressor in *A. thaliana* (Koguchi et al. 2017). FG repeat motif protein RanBP2 shown to be localized to cytoplasmic periphery of the nuclear pore complex (NPC), which plays a critical role in nuclear protein import (Delphin et al. 1997). It was also recently shown that NPC components play critical role in plant stress responses by regulating transcriptional genes and mRNA/protein nucleo-cytoplasmic trafficking (Yang et al. 2017). Similarly, a novel methionine aminopeptidase (HvMAP) has been reported to change its localization from nucleus to cytoplasm under low temperature to take part in freezing tolerance in *A. thaliana* (Jeong et al. 2011). Taken together, our findings of localization shift of AteIF4A-III and ALY4 from nucleus to cytoplasm and cytoplasmic periphery upon exposure to different abiotic stresses indicates the participation of these genes in multiple abiotic stress-responsive pathway.

AteIF4A-III DEAD-Box RNA Helicase Interacts with AtSTRS1 as a Stress-Responsive Indicator

Recent findings show that AteIF4A-III is involved in nuclear biogenesis activities mostly in the assembly of EJC (Koroleva et al. 2009b). Our study has also shown that functional activity of AteIF4A-III lies within nucleus as AteIF4A-III shows strong interaction with AtSTRS1 and the interaction was localized to nucleus. This indicates that AteIF4A-III and AtSTRS1 interact with each other under normal condition inside the nucleus involving in important nuclear cellular machinery. AteIF4A-III (ortholog of mammalian eIF4A-III) sub-cellular localization study reveals that these are involved in EJC assembly and interacts with other EJC core components like ALY/Ref, MAGO, Y14, and RNPS1, and under hypoxia, this interaction shifts from the nucleoplasm to the nucleolus and splicing speckles showing stress responsiveness (Koroleva et al. 2009b). Furthermore, it has been reported that FRY2/CPL1 interacts with two NMD factors, namely, AteIF4A-III and UPF3 to carry out degradation of NMD transcripts (Cui et al. 2016). Our present study for the first time reports the protein-protein interaction of AteIF4A-III and AtSTRS1 in vivo under normal and multiple abiotic stress conditions. The clear re-localization of AteIF4A-III and AtSTRS1 from nucleus to cytoplasm tested in both the directions under multiple abiotic stress conditions indicate that these two proteins are functionally associated in imparting multiple abiotic stress responses in *Arabidopsis*. The re-localization of these two interactors under stress also indicates that AteIF4A-III and AtSTRS1 coordinate with each other to suspend the biosynthesis

processes under different abiotic stress conditions. This might help the cell to escape from different abiotic stress conditions by moving towards cytoplasmic periphery. The localization shift of this interaction shows that their functional interaction is centralized on the nucleus. Whereas under stress conditions, AteIF4A-III and AtSTRS1 lowers the functions like cell cycle regulation, replication, RNA processing in the nucleus to save the energy of the cells under stressed conditions by shifting towards cytoplasm and cytoplasmic periphery. Since, AtSTRS1 has been known as abiotic stress negative regulator (Kant et al. 2007), it is highly likely that AteIF4A-III might also function as a negative regulator of different abiotic stresses in association with AtSTRS1 in *Arabidopsis*. As earlier explained, our sub-cellular localization results also showed the nuclear localization of AteIF4A-III under normal conditions and cytoplasmic re-localization under multiple abiotic stress conditions. AtSTRS1 is also known to be localized to nucleus under normal conditions from the previous study (Khan et al. 2014). Incidentally, our in silico protein-protein interaction analysis also showed the direct interaction of AteIF4A-III with AtSTRS1. For the in silico network, the search was restricted to only the 6 selected proteins based on the experimental data. Generally, the protein-protein interaction studies follow either of experimental or in silico methods. Most of the computational methods look into a system-wide interaction network which are based on high-throughput data. Though in the current study, the in silico method does not directly deal with high-throughput data and also is not a system-wide study, it has significant importance as the experimentally identified proteins of interest were the specific focus and the AraNet V2 (the database considered) incorporates huge omics datasets. Coming back to the findings from Fig. 6, establishment of interaction between AteIF4A-III and AtSTRS1 by both experimental and computational methods will be of special interest for our future study. Also, another interesting investigation will be to look into the interactions where the in vivo and in silico methods varied. The distribution of AteIF4A-III and AtSTRS-1 in the cytoplasm and poor signal in nucleoplasm under multiple abiotic stresses shows that ribosome and protein biosynthesis might have carried out at a very minimal level to save energy under different stress conditions. Taken together, we can infer that AteIF4A-III DEAD-box RNA helicase interacts with AtSTRS1 to regulate multiple abiotic stress responses.

AtALY4 Also Interacts with AteIF4A-III and AtSTRS1 In Vivo

Two orthologues of mammalian 54 UAP56-interacting factor (UIF), UIEF1, and UIEF2 mRNA export factor proteins interact with AtALY1-AtALY4 in *A. thaliana* for efficient nucleo-cytosolic mRNA transportation (Ehrnsberger et al. 2019). AtALY4 has also been considered as an important component of the EJC complex as it interacts with AteIF4A-III, MAGO, and Y14 EJC components (Pierrat et al. 2017; Boisramé et al. 2019). It was reported that there is functional interaction among AtALY1-4 mRNA export factor, RNA helicase UPA56, MOS11, TREX-2 mRNA export complex and other spliceosomal components (Sørensen et al. 2017; Naturwissenschaften 2016). In our study, the in silico analysis did not show any direct interaction of AtALY4 with either AteIF4A-III or AtSTRS1. On the

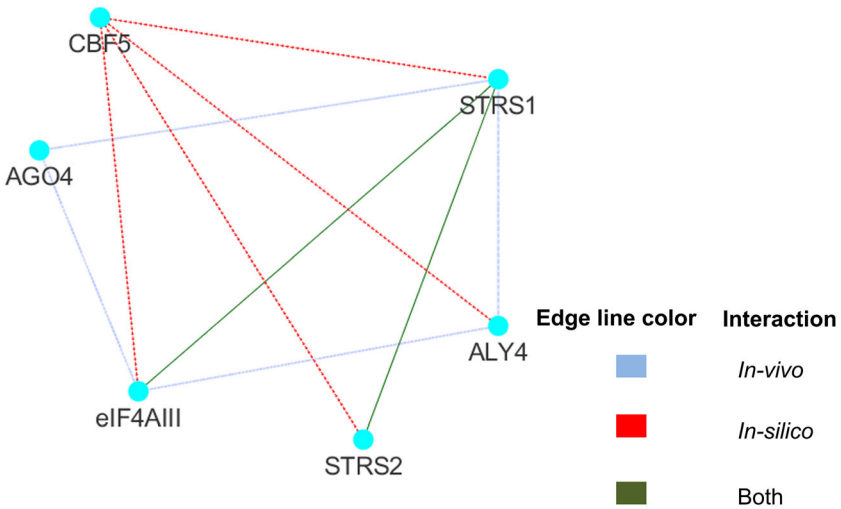

Fig. 6 Merged network of in silico and in vivo protein-protein interaction of DEAD-box RNA helicase proteins and their stress-associated proteins using Cytoscape software tool. Each node is representing a single DEAD-box RNA helicase and stress-associated proteins and each edge is representing interaction between two target proteins. The blue color edges indicate interaction from the in vivo split-YFP analysis, red color indicates interactions from in silico analysis and green color indicates interactions from both in vivo and in silico analysis. The network is of 6 nodes and 10 edges which represents the 6 proteins and 12 interactions (merged into 10 edges) among them. The network shows the interaction between AteIF4A-III and AtSTRS1; AtSTRS2 and AtSTRS1 from both in silico analysis and in vivo study

contrary, our in vivo split-YFP results have shown that AtALY4, an mRNA export factor, also showed direct interaction with AteIF4A-III and AtSTRS1 in one direction (Table 1) and the interaction pattern was not as strong as the interaction between AteIF4A-III and AtSTRS1. The stress-induced re-localization pattern of these interactors was similar to AteIF4A-III and AtSTRS1. Recent in silico data on AteIF4A-III interaction partners has shown that MAGO NASHI, RNA-binding protein Y14, nuclear distribution protein 1 (NDL1), nuclear pore complex protein (NUP43), and AtALY4 as its interacting partners (TAIR BioGRID database). Similarly, BioGRID information from TAIR database shows AtALY4 protein interacts with KIP2, MAGO, PARP1, Y14, AT5G02530, and AteIF4A-III. This information suggests that AteIF4A-III and AtALY4 are involved in nuclear assembly interacting with each other along with MAGO and Y14. It has been found that two homologous protein DIP1 and DIP2 (AtALY4) interacts with DNA-binding domain of plant poly (ADP-ribose) polymerase (PARP) which have a role in transcriptional regulation (Storozhenko et al. 2001). Often split-YFP results believed to show false positive or artifacts in interpreting the true interaction between the proteins. However, our systematic use of negative controls as described in the results for each of the binding partners did not show that any YFP signal has excluded the possibility of false positives or artifacts. Taken together, our in vivo interaction study also indicates that AtALY4 might also be functioning together with AteIF4A-III and AtSTRS1 in regulating multiple abiotic stress responses. In vivo results have strengthened our hypothesis to find out the role of DEAD-box genes, *AteIF4A-III* and *AtALY4*, in multiple abiotic stress response. However, our in silico and in vivo results are complimenting each other which was also shown in the protein-protein interaction network providing both in vivo and in silico information in the same network in Fig. 6. (Table 2)

Conclusions and Overview

The experimental findings have suggested that the functional site of AteIF4A-III, a DEAD-box RNA helicase, and putative mRNA export factor, AtALY4, is the nucleus. Since AteIF4A-III is known to be involved in RNP biogenesis, transcriptional to translational biogenesis and AtALY4 is involved in nucleo-cytosolic transfer of mRNA; it justifies our finding of sub-cellular localization of these two proteins in the nucleus. Transient multiple abiotic stress treatments revealed that both AteIF4A-III and AtALY4 are multiple stress-responsive. The

Table 1 Flow cytometry analysis of protein-protein interaction of AteIF4A-III, AtALY4, and stress-associated proteins

Sl. No.	Interacting Partners (both directions)	YFP fluorescence (%)*	Interaction type**
1	AtALY4$^{pE\text{-}SPYNE}$ X AteIF4A-III $^{pE\text{-}SPYCE}$	89.19	+
2	AteIF4A-III$^{pE\text{-}SPYNE}$ X AtALY4$^{pE\text{-}SPYCE}$	1.63	–
3	AteIF4A-III$^{pE\text{-}SPYNE}$ X AtAGO4 $^{pE\text{-}SPYCE}$	80.64	+
4	AtAGO4$^{pE\text{-}SPYNE}$ X AteIF4A-III $^{pE\text{-}SPYCE}$	79.52	+
5	AteIF4A-III$^{pE\text{-}SPYNE}$ X AtCBF5 $^{pE\text{-}SPYCE}$	0.04	–
6	AtCBF5$^{pE\text{-}SPYNE}$ X AteIF4A-III $^{pE\text{-}SPYCE}$	0.05	–
7	AteIF4A-III$^{pE\text{-}SPYNE}$ X AtSTRS1 $^{pE\text{-}SPYCE}$	85.39	+
8	AtSTRS1$^{pE\text{-}SPYNE}$ X AteIF4A-III $^{pE\text{-}SPYCE}$	84.90	+
9	AteIF4A-III$^{pE\text{-}SPYNE}$ X AtSTRS2 $^{pE\text{-}SPYCE}$	0.04	–
10	AtSTRS2$^{pE\text{-}SPYNE}$ X AteIF4A-III $^{pE\text{-}SPYCE}$	0.011	–
11	AtALY4$^{pE\text{-}SPYNE}$ X AtAGO4 $^{pE\text{-}SPYCE}$	0.04	–
12	AtAGO4$^{pE\text{-}SPYNE}$ X AtALY4 $^{pE\text{-}SPYCE}$	0.06	–
13	AtALY4$^{pE\text{-}SPYNE}$ X AtCBF5 $^{pE\text{-}SPYCE}$	0.11	–
14	AtCBF5$^{pE\text{-}SPYNE}$ X AtALY4 $^{pE\text{-}SPYCE}$	0.07	–
15	AtALY4$^{pE\text{-}SPYNE}$ X AtSTRS1 $^{pE\text{-}SPYCE}$	87.01	+
16	AtSTRS1$^{pE\text{-}SPYNE}$ X AtALY4 $^{pE\text{-}SPYCE}$	79.72	+
17	AtALY4$^{pE\text{-}SPYNE}$ X AtSTRS2 $^{pE\text{-}SPYCE}$	0.05	–
18	AtSTRS2$^{pE\text{-}SPYNE}$ X AtALY4 $^{pE\text{-}SPYCE}$	0.05	–
19	pE-SPYCE x pE-SPYNE (empty vector)	0.04	–

*% represents how many protoplast cells have shown YFP positive signal out of the total number of cells tested in flow cytometry

**"+" represents positive interaction; "–" represents negative interaction

Table 2 Comparison of in silico and in vivo protein-protein interactions of AteIF4A-III, AtALY4, and stress-associated proteins

Sl. No.	Interacting Partners (both directions)	In silico	In vivo	Both*
1	AteIF4A-III-YFP^N X AtALY4-YFP^C	−	−	−
2	AteIF4A-III-YFP^C X AtALY4-YFP^N	−	+	−
3	AteIF4A-III-YFP^N X AtAGO4-YFP^C	−	+	−
4	AteIF4A-III-YFP^C X AtAGO4-YFP^N	−	+	−
5	AteIF4A-III-YFP^N X AtCBF5-YFP^C	+	−	−
6	AteIF4A-III-YFP^C X AtCBF5-YFP^N	+	−	−
7	AteIF4A-III-YFP^N X AtSTRS1-YFP^C	+	+	+
8	AteIF4A-III-YFP^C X AtSTRS1-YFP^N	+	+	+
9	AteIF4A-III-YFP^N X AtSTRS2-YFP^C	−	−	−
10	AteIF4A-III-YFP^C X AtSTRS2-YFP^N	−	−	−
11	AtALY4-YFP^N X AtAGO4-YFP^C	−	−	−
12	AtALY4-YFP^C X AtAGO4-YFP^N	−	−	−
13	AtALY4-YFP^N X AtCBF5-YFP^C	+	−	−
14	AtALY4-YFP^C X AtCBF5-YFP^N	+	−	−
15	AtALY4-YFP^N X AtSTRS1-YFP^C	−	+	−
16	AtALY4-YFP^C X AtSTRS1-YFP^N	−	+	−
17	AtALY4-YFP^N X AtSTRS2-YFP^C	−	−	−
18	AtALY4-YFP^C X AtSTRS2-YFP^N	−	−	−

*"+" represents positive interaction; "–" represents negative interaction

systematic in vivo split-YFP analysis under normal and multiple abiotic stress conditions revealed that AteIF4A-III, AtALY4, and AtSTRS1 functioning together in regulating responses to multiple abiotic stresses. Detailed genetic interaction in stable *Arabidopsis* lines through triple-gene CRISPR/Cas9 genome editing of AteIF4A-III, AtALY4, and AtSTRS1 and downstream functional characterization would reveal the mechanistic role of these genes in multiple abiotic stress regulation in plants. Understanding the mechanistic role of these key proteins in multiple abiotic stress responses is highly significant in developing sustainable multi-stress tolerance in crop plants in future. This would sustain the crop productivity under rapidly changing global climate.

Acknowledgments The authors would acknowledge the Director of CSIR-NEIST, Jorhat, for the facility and lab space.

Author Contributions IB performed Gateway construct designing, isolation of protoplast, transient sub-cellular localization, flow cytometry study, phylogenetic analysis, data analysis, and drafting of the manuscript. GB and JS have contributed the in silico studies, comparison of in silico, and in vivo interaction analysis in the manuscript. DLS, HPDB, NV, and CC revised the manuscript and provided critical inputs. CC designed the project concept, critically corrected the manuscript, evaluated and supervised the entire study.

Funding Information The work was funded by the Science and Engineering Research Board, Department of Science and Technology, New Delhi, India (SERB-DST), Govt. of India Grant Code: SB/S2/RJN-078/2014 as Ramanujan Fellowship and Grant Code: ECR/2016/001288 as Early Career Research Award to Channakeshavaiah Chikkaputtaiah. The author also wants to acknowledge the Human Resource Development Group, Council of Scientific and Industrial Research (CSIR), Govt. of India for funding Indrani Baruah as Senior Research Fellow (SRF-Direct).

Compliance with Ethical Standards

Conflict of Interest The authors declare that they have no conflict of interest.

Abbreviations AtALY4, Always Early 4; AtAGO4, Argonaute RISC component 4; AtSTRS1, Stress Response Suppressor 1; CRISPR/Cas9, clustered regularly interspaced short palindromic repeats and CRISPR-associated protein 9; CRISPR/Cpf1F, clustered regularly interspaced short palindromic repeats from Prevotella and Francisella 1; CBF, core-binding factor; AteIF4A-III, Eukaryotic Initiation Factor 4A-III; DREB, dehydration responsive element-binding protein); FAO, Food and Agricultural Organization; ESTs, expressed sequence tags; EJC, exon junction complex; MOS11, MODIFIER OF SNC1, 11; PDH45, pea DNA helicase 45; QTLs, quantitative trait locus; ROS, reactive oxygen species; SNPs, single-nucleotide polymorphisms; TILLING, Targeting Induced Local Lesions in Genomes; TALEN, Transcription activator-like effector nucleases; ZFN, Zinc-finger nucleases

References

Andreou AZ, Klostermeier D (2013) The DEAD-box helicase eIF4A: paradigm or the odd one out? RNA Biol 10:19–32

Barak S, Farrant JM (2016) Extremophyte adaptations to salt and water deficit stress. Func Plant Biol 43,v–x

Baruah I, Debbarma J, Boruah HPD, Keshavaiah C (2017) The DEAD-box RNA helicases and multiple abiotic stresses in plants: a systematic review of recent advances and challenges. PLANT OMICS 10: 252–262

Boisramé A, Devillers H, Onésime D, Brunel F, Pouch J, Piot M, Neuvéglise C (2019) Exon junction complex components Y14 and Mago still play a role in budding yeast. Sci Rep 9:849

Chikkaputtaiah C, Debbarma J, Baruah I, Havlickova L, Deka Boruah HP, Curn V (2017) Molecular genetics and functional genomics of abiotic stress-responsive genes in oilseed rape (Brassica napus L.): a review of recent advances and future. Plant Biotech Rep 11:365–384

Cui P, Chen T, Qin T, Ding F, Wang Z, Chen H, Xiong L (2016) The RNA polymerase II C-terminal domain phosphatase-like protein FIERY2/CPL1 interacts with AteIF4A-III and is essential for nonsense-mediated mRNA decay in Arabidopsis. Plant Cell 28:770–785

da-Silva TL, Roseiro JC, Reis A (2012) Applications and perspectives of multi-parameter flow cytometry to microbial biofuels production processes. TrendsBiotechnol 30:225–232

Debbarma J, Sarki YN, Saikia B, Deka Boruah HP (2019) Ethylene response factor (ERF) family proteins in abiotic stresses and CRISPR–Cas9 genome editing of ERFs for multiple abiotic stress tolerance in crop plants : a review. Mol Biotechnol 61:153–172

Delphin C, Guan T, Melchior F, Gerace L (1997) RanGTP targets p97 to RanBP2, a filamentous protein localized at the cytoplasmic periphery of the nuclear pore complex. Mol Biol Cell 8:2379–2390

Donoghue MTA, Keshavaiah C, Swamidatta SH, Spillane C (2011) Evolutionary origins of Brassicaceae specific genes in Arabidopsis thaliana. BMC Evol Biol 11:1–23

Ehrnsberger HF, Pfaff C, Hachani I, Flores-Tornero M, Sørensen BB, Längst G, Sprunck S, Grasser M, Grasser KD (2019) The UAP56-interacting export factors UIEF1 and UIEF2 function in mRNA export. Plant Physiol 179:1525–1536

FAO (2017) FAOSTAT. Food and Agriculture Organization of the United Nations, Rome

Freye ECK, Strobel HP (2018) Coenzyme Q10 supplements which increase ATP synthesis within mitochondria and protect against toxic sodium Azide. Acta Sci Nut Health 2:2–9

Ghosh MK (2019) The emerging roles of the DEAD box RNA helicase p68 in oncogenesis. Acta Sci Cancer Biol 3:10–11

Han F, Sun M, He W, Cui X, Pan H, Wang H, Song F, Lou Y, Zhuge Y (2019) Ameliorating effects of exogenous Ca 2 + on foxtail millet seedlings under salt stress. Func Plant Biol 46:407–416

Hasanuzzaman AM, Shabala L, Tim JB, Zhou M, Shabala S (2016) Assessing the suitability of various screening methods as a proxy for drought tolerance in barley. Func Plant Biol. 44:253. https://doi.org/10.1071/FP16263

Hellal FA, El-shabrawi HM, El-hady MA, Khatab IA, El-Sayed SAA, Abdelly C (2017) Influence of PEG induced drought stress on molecular and biochemical constituents and seedling growth of Egyptian barley cultivars. J Genet Eng Biotech 16:203–212

Herzenberg LA, Tung J, Moore WA, Herzenberg LA, Parks DR (2006) Interpreting flow cytometry data: a guide for the perplexed. Nat Immunol 7:681–685

Huang C, Sie YS, Chen YF, Huang TS, Lu CA (2016) Two highly similar DEAD box proteins , OsRH2 and OsRH34 , homologous to eukaryotic initiation factor 4AIII , play roles of the exon junction complex in regulating growth and development in rice. BMC Plant Biol 16:1–15

Jeong HJ, Jeong SS, Ok SH (2011) Barley DNA-binding methionine aminopeptidase, which changes the localization from the nucleus to the cytoplasm by low temperature, is involved in freezing tolerance. Plant Sci 180(1):53–60

Kammel C, Thomaier M, Sørensen BB, Schubert T, Längst G, Grasser M, Grasser KD (2013) Arabidopsis DEAD-box RNA helicase UAP56 interacts with both RNA and DNA as well as with mRNA export factors. PLoS One 8:e60644. https://doi.org/10.1371/journal.pone.0060644

Kant P, Kant S, Gordon M, Shaked R, Barak S (2007) STRESS RESPONSE SUPPRESSOR1 and STRESS RESPONSE SUPPRESSOR2, two DEAD-box RNA helicases that attenuate Arabidopsis responses to multiple abiotic stresses. Plant Physiol 145:814–830

Keunen E, Remans T, Bohler S, Vangronsveld J, Cuypers A (2011) Metal-induced oxidative stress and plant mitochondria. Int J Mol Sci 12(10):6894–6918

Khan A, Garbelli A, Grossi S, Florentin A, Batelli G, Acuna T, Zolla G, Kaye Y, Paul LK, Zhu JK, Maga G, Grafi G, Barak S (2014) The Arabidopsis STRESS RESPONSE SUPPRESSOR DEAD-box RNA helicases are nucleolar- and chromocenter-localized proteins that undergo stress-mediated relocalization and are involved in epigenetic gene silencing. Plant J 79:28–43

Kiełkowska A, Grzebelus E, Lis-Krzyścin A, Maćkowska K (2019) Application of the salt stress to the protoplast cultures of the carrot (Daucus carota L.) and evaluation of the response of regenerants to soil salinity. Plant Cell Tissue Organ Cult 137:379–395

Koguchi M, Yamasaki K, Hirano T, Sato MH (2017) Vascular plant one-zinc-finger protein 2 is localized both to the nucleus and stress granules under heat stress in Arabidopsis. Plant Signal Behav 12(3):e1295907

Kollárová K, Kusá Z, Vatehová-Vivodová Z, Lišková D (2019) The response of maize protoplasts to cadmium stress mitigated by silicon. Ecotoxicol Environ Saf 170:488–494

Koroleva OA, Brown JW, Shaw PJ (2009a) Localization of eIF4A-III in the nucleolus and splicing speckles is an indicator of plant stress. Plant Signal Behav 4:1148–1151

Koroleva OA, Calder G, Pendle AF, Kim SH, Lewandowska D, Simpson CG, Jones IM, Brown JW, Shaw PJ (2009b) Dynamic behavior of Arabidopsis eIF4A-III, putative core protein of exon junction complex: fast relocation to nucleolus and splicing speckles under hypoxia. Plant Cell 21:1592–1606

Krasikov V, Dekker HL, Rep M, Takken FL (2011) The tomato xylem sap protein XSP10 is required for full susceptibility to Fusarium wilt disease. J Exp Bot 62(3):963–973

Liu Y, Tabata D, Imai R (2016) A cold-inducible DEAD-box RNA helicase from arabidopsis thaliana regulates plant growth and development under low temperature. PLoS One 11:1–21

Lu W, Wilczynska A, Smith E, Bushell M (2014) The diverse roles of the eIF4A family : you are the company you keep. Biochem Soc Trans 42:166–172

Lycoskoufis I, Mavrogianopoulos G, Savvas D, Ntatsi G (2012) Impact of salinity induced by high concentration of NaCl or by high concentration of nutrients on tomato plants. Acta Hort 952:689–696

Marwein R, Debbarma J, Sarki YN, Baruah I, Saikia B, Deka Boruah HP, Velmurugan N, Chikkaputtaiah C (2019) Genetic engineering/genome editing approaches to modulate signaling processes in abiotic stress tolerance. In: Plant Signalling molecules, 1st edn. ELSEVIER Publishers, Germany, pp 63–82

Naturwissenschaften DDER (2016) Molecular and functional characterization of the THO/TREX complex in Arabidopsis thaliana. Dissertation, Biology and preclinical medicine of the University of Regensburg, Herning, Denmark

Nawaz G, Kang H (2019) Rice OsRH58 , a chloroplast DEAD-box RNA helicase , improves salt or drought stress tolerance in Arabidopsis by affecting chloroplast translation. BMC Plant Biol 19:1–11

Nawaz G, Lee K, Park SJ, Kim YO, Kang H (2018a) A chloroplast-targeted cabbage DEAD-box RNA helicase BrRH22 confers abiotic stress tolerance to transgenic Arabidopsis plants by affecting translation of chloroplast transcripts. Plant Physiol Biochem 127:336–342

Nawaz G, Zaw T, Sai T, Lee K, Kim YO, Kang H (2018b) Rice DEAD-box RNA helicase OsRH53 has negative impact on Arabidopsis response to abiotic stresses. Plant Growth Regul 85:153–163

Nguyen LV, Seok H, Woo D, Lee S, Moon Y (2018) Overexpression of the DEAD-box RNA helicase gene AtRH17 confers tolerance to salt stress in Arabidopsis. Int J Mol Sci 19:1–16

Ohad N, Shichrur K, Yalovsky S (2007) The analysis of protein-protein interactions in plants by bimolecular fluorescence complementation. Plant Physiol 145:1090–1099

Pascuan C, Frare R, Alleva K, Ayub ND, Soto G (2016) mRNA biogenesis-related helicase AteIF4A-III from Arabidopsis thaliana is an important factor for abiotic stress adaptation. Plant Cell Rep 35: 1205–1208

Pfaff C, Ehrnsberger HF, Flores-tornero M, Sørensen BB, Schubert T, Längst G, Griesenbeck J, Sprunck S, Grasser M, Grasser KD (2018) ALY RNA-binding proteins are required for nucleocytosolic mRNA transport and modulate plant growth and development. Plant Physiol 177:226–240

Pierrat OA, Paudyal A, Woodruff J, Koroleva O, Boateng SY (2017) The exon junction complex senses energetic stress and regulates contractility and cell architecture in cardiac myocytes. Biosci Rep 37:1–13

Powers SK, Holehouse AS, Korasick DA, Jez JM, Pappu RV, Strader LC (2019) Nucleo cytoplasmic partitioning of ARF proteins controls auxin responses in Arabidopsis thaliana. Mol Cell 76(1):177–190

Rao TSRB, Naresh JV, Reddy PS, Reddy MK, Mallikarjuna G (2017) Expression of Pennisetum glaucum eukaryotic translational initiation factor 4A (PgeIF4A) confers improved drought, salinity, and oxidative stress tolerance in groundnut. Front Plant Sci 8:1–15

Rivero L, Scholl R, Holomuzki N, Crist D, Grotewold E, Brkljacic J (2014) Handling Arabidopsis plants: growth, preservation of seeds, transformation, and genetic crosses. Methods Mol biol (Clifton, N.J.) 1062:3–25

Shivakumara TN, Sreevathsa R, Dash PK, Sheshshayee MS, Papolu PK, Rao U, Tuteja N, UdayaKumar M (2017) Overexpression of Pea DNA Helicase 45 (PDH45) imparts tolerance to multiple abiotic stresses in chili (*Capsicum annuum* L .). Sci Rep 7:1–12

Slaine PD, Kleer M, Smith NK, Khaperskyy DA, McCormick C (2017) Stress granule-inducing eukaryotic translation initiation factor 4A inhibitors block influenza a virus replication. Viruses 9:1–15

Sørensen BB, Ehrnsberger HF, Esposito S, Pfab A, Bruckmann A, Hauptmann J, Meister G, Merkl R, Schubert T, Längst G, Melzer M, Grasser M, Grasser KD (2017) The Arabidopsis THO/TREX component TEX1 functionally interacts with MOS11 and modulates mRNA export and alternative splicing events. Plant Mol Biol 93: 283–298

Storozhenko S, Inzé D, Van Montagu M, Kushnir S (2001) Arabidopsis coactivator ALY-like proteins , DIP1 and DIP2 , interact physically with the DNA-binding domain of the Zn-finger poly(ADP-ribose) polymerase. J Exp Bot 52:1375–1380

Tao S, Jiao Z, Wen G, Zhang L, Wang G (2018) Cloning and expression analysis of the DEAD- box/RNA helicase Oslaf-1 in Ovomermis sinensis. PLoS One 13:e0192101. https://doi.org/10.1371/journal.pone.0192101

Teng W, Zhang H, Wang W, Li D, Wang M, Liu J, Zhang H, Zheng X, Zhang Z (2014) ALY proteins participate in multifaceted Nep1Mo-triggered responses in Nicotiana benthamiana and Arabidopsis thaliana. J Exp Bot 65:2483–2494

Uhrig JF, Canto T, Marshall D, Macfarlane SA (2004) Relocalization of nuclear ALY proteins to the cytoplasm by the tomato bushy stunt virus P19 pathogenicity protein. Plant Physiol 135:2411–2423

Vandromme M, Gauthier-Rouvière C, Lamb N, Fernandez A (1996) Regulation of transcription factor localization: fine-tuning of gene expression. Trends Biochem Sci 21:59–64

Wang W, Lin Y, Teng F, Ji D, Xu Y, Chen C, Xie C (2018) Comparative transcriptome analysis between heat-tolerant and sensitive Pyropia haitanensis strains in response to high temperature stress. Algal Res 29:104–112

Yadav S, Tuteja N (2019) Molecular and functional insights in 'helicases from all domains of life'. In: Tuteja R (ed) Evolution of RNA helicases in plants, 1st edn. Academic Press, New Delhi, pp 53–75

Yang Z, Li H, Guo D, Peng S (2016) Identification and characterization of MAGO and Y14 genes in Hevea brasiliensis. Genet Mol Biol 39: 73–85

Yang Y, Wang W, Chu Z, Zhu JK, Zhang H (2017) Roles of nuclear pores and nucleo-cytoplasmic trafficking in plant stress responses. Front Plant Sci. https://doi.org/10.3389/fpls.2017.00574

Yoo SD, Cho YH, Sheen J (2007) Arabidopsis mesophyll protoplasts : a versatile cell system for transient gene expression analysis. Nat Prot 2:1565–1573

Zhu M, Chen G, Dong T, Wang L, Zhang J, Zhao Z, Hu Z (2015) SlDEAD31, a putative 593 DEAD-box RNA helicase gene, regulates salt and drought tolerance and stress-related 594 genes in tomato. PLoS One 10:e0133849. https://doi.org/10.1371/journal.pone.0133849